

# Dynamic Analysis on the Safety Criteria of the Conceptual Core Design in MTR Type Research Reactor

## ARTICLE INFO

### AIJ use only:

Received date

Revised date

Accepted date

### Keywords:

MTR type research reactor, control rod velocity, high uranium density, MTR-DYN code

## ABSTRACT

A research activity with high priority in Batan is designing a new research reactor MTR type with a new fuel. The core is compact core model that consists of 16 fuels and 4 control rods. The high-density uranium fuel will increase the cycle length of the reactor operation but the compact core model will also increase the heat flux in the reactor core. The increasing heat flux at the fuel will cause the temperature of the fuel and cladding increase so that the coolant flow rate could be increased. However, the coolant flow rate in the fuel element has a limit value due to the thermal hydraulic stability in the core. Therefore, the dynamic analysis is important in evaluating design and operation of nuclear reactor safety. The objective of this research work is to carry out a dynamic analysis for a conceptual core of MTR research reactor fuelled with the low enrichment U9Mo-Al dispersion with 390 uranium fuel loading (3.96 gram/cc). The calculations were performed using WIMSD-5B, Batan-2DIFF, Batan-3DIFF, POKDYN, and MTRDYN codes. The WIMSD-5B code was used for generating the group constants of all core materials. The neutronics and kinetics parameter such as keff, PPF, the core reactivity balance, coefficient reactivity were calculated by Batan-2DIFF code and control rod reactivity worth was calculated by Batan-3DIFF code. POKDYN code is used to determine the maximum control rod speed. Steady state thermal hydraulic parameters and dynamic analysis were determined using the MTRDYN code. The calculation results showed that the core reactivity balance, reactivity coefficient and also control rod reactivity worth meet the safety criteria. Using the dynamic analysis, the maximum control rod speed is achieved as 0,0846 cm/s. The maximum temperatures of the coolant, cladding and fuel meat with the uranium density of 3,96 g/cc are 76.01°C, 192.02°C and 196.24°C, respectively. The maximum value of fuel meat temperature for safety limit is 2100C, it means that the maximum temperatures fulfilled the design limit, therefore, the reactor has a safe operation at the nominal power. The dynamic analysis showed that inherently safety can save the operation reactor when insertion of reactivity occurs in the core.

© 2010 Atom Indonesia. All rights reserved

## INTRODUCTION

One of research activity with high priority in the Center for Nuclear Reactor Technology and Safety-Batan is to design new research reactor using uranium-molybdenum fuel (U-9Mo/Al). High loading of fissile material in the U-9Mo/Al fuel is expected to increase the operation cycle; hence, higher reactor availability and utilization can be achieved while the fuel cost can be reduced[1].

An early conceptual design of Material Testing Reactor (MTR) type from neutronics aspect has been derived by T. Surbakti., et al.[2] with main characteristics of core configuration as specified as

follow. The RRI research reactor has a nominal power of 20 MW, uses a uranium-molybdenum alloy, U-9Mo/Al fuel with geometry adopting from RSG-GAS' fuel. The core configuration in 5 x 5 lattice is made up of 20 fuel elements and 5 irradiation positions and produces thermal neutron flux in the order of  $2.87 \times 10^{14}$  neutron  $\text{cm}^{-2} \text{s}^{-1}$ . This neutron flux value is still lower than one stated as acceptance criteria of MTR type reactor in which the reactor should have a maximum neutron flux in irradiation positions and in the reflector region with high thermal neutron flux at least in the order of  $1.0 \times 10^{15}$  and  $0.5 \times 10^{15}$  neutron  $\text{cm}^{-2} \text{s}^{-1}$ , respectively.

The second conceptual design was proposed by I. Kuntoro. et al.[3] where the grid core is the same but the height of the fuel and power are

\* Corresponding author.  
E-mail address:

44different. To fulfill that acceptance criterion, the 100calculations. This section elaborates these two  
45core was designed with the fuel elements 70 cm of 101calculation types.

46height and the power level of 50 MW and the 102

47others size are the same with the lattices of reactors 103A.

### Cell calculation

48which previously design. The core configuration is 104

49specified by the number and positions of fuel 105To solve the neutron kinetics equations, the  
50elements and irradiation positions. After finding the 106macroscopic cross section library for various

51optimum core configuration met the acceptance 107materials in the core is set-up. For this purpose, the  
52criteria that the value of neutron flux in the center of 108WIMSD-5B lattice code is used. In practice, the

53the core is not less than  $1.0 \times 10^{15}$  n/cm<sup>2</sup> s, it is 109cells which may correspond to any region of the  
54necessary to analyze the dynamic of the core to 110core (fueled and non-fueled) are identified. When

55understand the characteristic of the core from safety 111defining the unit cell dimensions, the principle of  
56feature. However, dynamic analysis has not been 112conservation of volume ratio of the different

57done for this MTR conceptual core design. For this 113material in the fuel assembly is considered. The  
58purpose, the conceptual core design is considered in 114fuel assembly in the core configuration is showed in

59a transient condition. The calculation concern for 115Figure 1. The fuel cell dimensions are calculated  
60rapid transient initiated by positive reactivity 116taking into account the fuel meat conservation

61induced accident during a control rod withdrawal at 117criteria. The unit cell for fuel element (FE) is  
62the power of 1 MW. Many researches have 118showed in Figure 2. An extra region is added

63performed neutronic and thermal-hydraulic 119accounting for the remaining water and aluminum in  
64calculations to understanding the safety features for 120the same proportions as in the physical fuel element

65research reactor using PARET, RELAP, COOLOD- 121, this region includes the aluminum in the plates  
66N2 and EUREKA codes.[4,5,6,7,8] but for this 122beyond the width of the meat and the aluminum side

67research using MTR-DYN code. 123plates, the water beyond the width of the meat, and  
68

69 This research is a subsequent evaluation 124the water channels surrounding the fuel element. In  
70design for conceptual core design of MTR research 125the particular case of control element, the super-cell

71reactor by focusing on identifying safety limit and 126option of WIMSD-5B is used. The representative  
72margin. In this research is discussed the dynamic 127cell is modeled with 15 regions. The control rod and

73analysis for conceptual core design of MTR research 128box absorber are showed in Figure 3 and 4. The  
74reactor used MTR-DYN code[9]. Before the 129macroscopic cross-section data were generated by  
75analysis is done, it was started from design 130WIMSD-5B code as a function of burn-up and fuel

76calculations and carried out by means of WIMSD- 131and moderator temperatures. Different burn-up  
765B[10] for cross-section generation as an input to 132values, ranging from 0% to 90 % were considered in

77Batan-3DIFF diffusion code for core 133order to generate all conditions, beginning of cycle  
78calculation[11] to determine the integral and 134and end of cycle cores.

79differential control rod worth. The macroscopic 135

80cross-section was also needed to calculate the fuel 136Fuel and moderator temperatures were chosen in  
81and moderator reactivity coefficient and delayed 137order to cover a large set of core condition for

82neutron fraction. To determining the maximum 138normal and transient conditions. The macroscopic  
83speed of control, it is used a period-reactivity 139cross-section also was performed to determine the

84relation. The MTR-DYN code is used to determine 140average speed of neutrons. The cross-section  
85the thermal-hydraulic parameter to analyze core 141generation is done actually in 4 neutron energy

86dynamic as a rapid transient initiated by positive 142group, but in the determination of the average speed  
87reactivity in the core. 143of neutrons is carried out in 69 group neutron

88 The WIMSD-5B code is used for calculating 144energy. The average speed of neutrons in 4 groups  
89group constants for different materials in the MTR 145of power calculated by weighting the speed of

90type research reactor core. Batan-3DIFF and MTR- 146neutrons in 69 energy groups with a average cell  
91DYN codes are used for core calculation. These 147flux. The speed of neutron was used to calculate

92codes which used for the neutronics and steady state 148total delayed neutron fraction.

93thermal hydraulic and dynamic parameters which 149

94had been verified using RSG-GAS core[12]. 150

Steps of cell calculation are as follows:[13]

95

151a. The macroscopic x-section as a function of burn-

## METHODOLOGY

152 up is generated under ambient conditions (20°C).

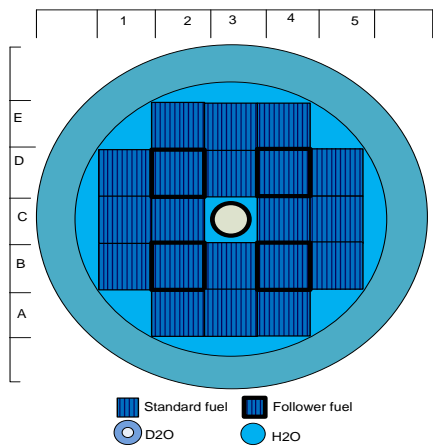
96

153b. The macroscopic x-section for fuel elemen

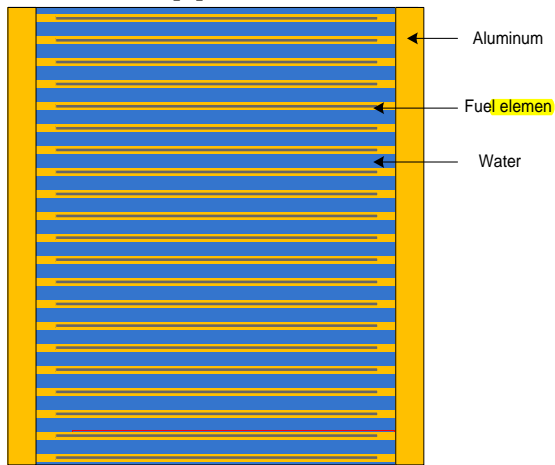
97 The methodology to achieve the research 154 is generated as a function of temperatures (50°C,

98 objective can be divided into two types of 155 100°C, 150°C, 200°C).

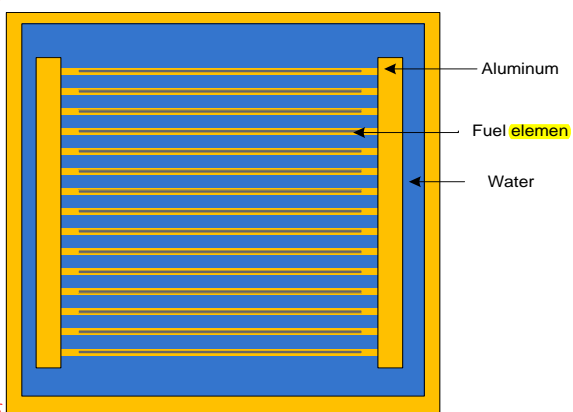
156c. The macroscopic x-section for moderator is  
 157 generated as a function of temperatures (35°C,  
 158 45°C, 60°C, 100°C). In this step the moderator  
 159 density unchanged



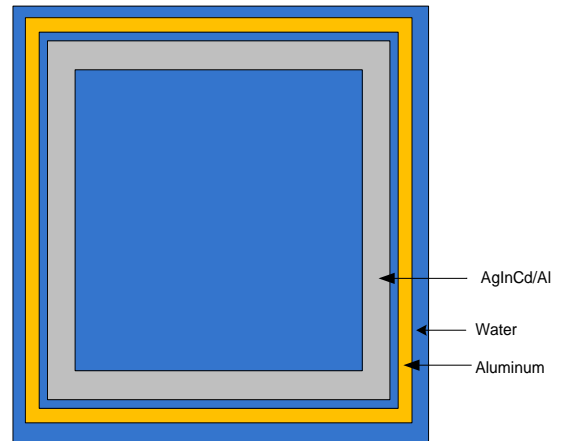
160 Fig. 1. Core configurations of the MTR type  
 161 research reactor [2]



163 Fig. 2. Standard fuel element [2]



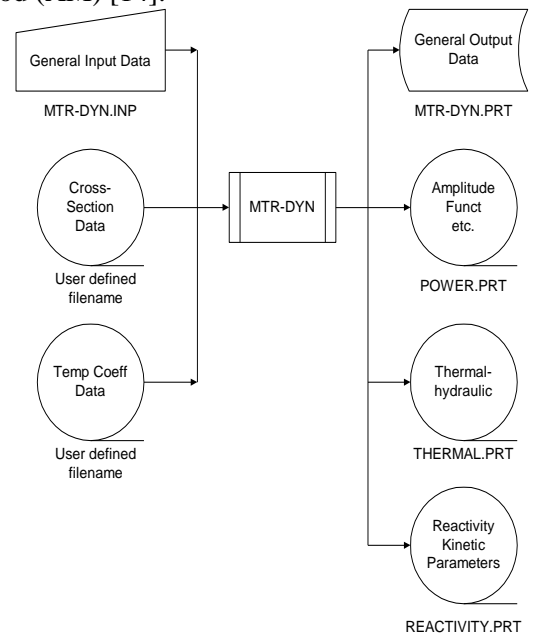
166 Fig. 3. Fuel follower element [2]



169 Fig. 4. Control rod element [2]

170  
 171  
 172 **B. Core calculation**

173  
 174 Core calculation was done by using Batan-2  
 175 DIFF and Batan-3DIFF codes for coefficient  
 176 reactivity, integral and differential control rod  
 177 worth. Batan-2DIFF was also used to calculate total  
 178 delayed neutron fraction which is needed as an  
 179 input for MTR-DYN code for dynamic analysis.  
 180 The MTR-DYN code is a coupled neutronic (N) and  
 181 thermal-hydraulic (T/H) code for the MTR research  
 182 reactor type. This code is developed using 3-  
 183 dimensional multigroup neutron diffusion with  
 184 finite difference method. Flowchart of N and steady  
 185 state T/H calculations are shown in Figure 5. All  
 186 calculations were carried out by the adiabatic  
 187 method (AM) [14].



188 Fig. 5. MTR-DYN code input/output file structure  
 189 [14]

190  
 191  
 192  
 193  
 194

195 **RESULTS AND DISCUSSION**

196  
 197 Neutronic parameter of MTR type research reactor  
 198 are showed in Table 1. The result showed that the  
 199 radial power peaking factor (PPF) value <1.4, as  
 200 well as the maximum neutron flux in the center of  
 201 the core already met the acceptance criteria > 1.0 x  
 202 10<sup>15</sup> n / cm<sup>2</sup>s. The value of the PPF on the  
 203 equilibrium core is far below the safety limit. The  
 204 PPF value will change due to the pattern and  
 205 materials exchange in the core. It can be said that  
 206 the PPF is affected by fuel management. Therefore  
 207 the primary factor in determining the maximum  
 208 value of PPF is a burn-up distribution in the fuels  
 209 and around the control rod positions. Radial PPF  
 210 greatest value is 1.24 with the largest fraction and is  
 211 close to the control rod (D-2) position at equilibrium  
 212 core. The maximum radial PPF value is less than the  
 213 value of safety limit 1.4.

214 Table 1. Neutronic parameters of MTR research  
 215 reactor  
 216

No.	Parameters	Uranium density 3.96 [gU/cm <sup>3</sup> ]
1.	Excess reactivity[%Δk/k]	11.32
2.	Contol rod worth [%Δk/k]	-25.60
3.	Maximum radial power peaking factor	1.23
4.	Cycle length reactor operation (days)	15
5.	Maximum axial power peaking factor	2.1
6.	Maximum thermal neutron flux in the irradiation position (E15 n/cm <sup>2</sup> s)	0.579
7.	Maximum thermal neutron flux in the center (E15 n/cm <sup>2</sup> s)	1.08
8.	Power density (W/cm <sup>3</sup> )	635

217  
 218 **a. Reactor kinetic parameter**

219  
 220 Reactor kinetic parameter such as delayed neutron  
 221 fraction and prompt neutron lifetime are needed to  
 222 determine for dynamic analysis. Table 2 showed  
 223 that calculation result of delayed neutron fraction  
 224 and prompt neutron lifetime for research reactor  
 225 MTR type using U9Mo-Al fuel with 3.96 g/cc of  
 226 density. The bigger delayed neutron fraction is the  
 227 easier for the core to be controlled when the  
 228 transient occurs in the reactor. Compare the value  
 229 with the RSG-GAS core is 7.16 E-03. Reactor  
 230 kinetics parameters required in this study was  
 231 effective delayed neutron fraction (β<sub>k</sub>) and

232 delayed neutron decay constant. Acceptance criteria  
 233 for a kinetic parameter value such as effective  
 234 delayed neutron fraction (β<sub>eff</sub>) is β<sub>eff</sub> = γ β, (γ = 1.05  
 235 to 1.25) and the value β is 0.0064 for uranium  
 236 fuel[15]. So the value of the effective delayed  
 237 neutron fraction total should be in the range of  
 238 0.00672 to 0.00840. Beyond this value, the kinetic  
 239 parameters β<sub>eff</sub> will be rejected.

240  
 241 Table 2. delayed neutron fraction for density of 3.96  
 242 gram/cc

Group	Delayed neutron fraction (β <sub>k</sub> )	Decay constant of delayed neutron (λ <sub>k</sub> ) s <sup>-1</sup>
1	2.61123.10 <sup>-04</sup>	1.29065.10 <sup>-02</sup>
2	1.53233.10 <sup>-03</sup>	3.11613.10 <sup>-02</sup>
3	1.69042.10 <sup>-03</sup>	1.34027.10 <sup>-01</sup>
4	2.65407.10 <sup>-03</sup>	3.31390.10 <sup>-01</sup>
5	7.56494.10 <sup>-04</sup>	1.46117.10 <sup>-00</sup>
6	2.95836.10 <sup>-04</sup>	3.81104.10 <sup>+00</sup>
Total delayed neutron fraction :		7.19027.10 <sup>-03</sup>
Average decay constant :		7.84863.10 <sup>-02</sup> s <sup>-1</sup>
Prompt neutron lifetime :		55.49.10 <sup>-6</sup> s

243  
 244 It is important to know the sign and magnitude of  
 245 the various reactivity coefficients because these  
 246 coefficients suggest the consequences of sudden  
 247 changes in the operating parameters. A positive  
 248 value for a reactivity coefficient means that a  
 249 positive change in that parameter will increase  
 250 reactivity and tend to increase power. A negative  
 251 value for a reactivity coefficient means that a  
 252 positive change in that parameter will decrease  
 253 reactivity and tend to decrease power. In both cases,  
 254 a larger absolute value of the reactivity coefficient  
 255 becomes greater sensitivity to changes in that  
 256 parameter. Batan-2DIFF code calculates accurately  
 257 the fuel and moderator temperature coefficient of  
 258 reactivity. The calculation result in Table 3 showed  
 259 that the moderator temperature reactivity coefficient  
 260 is negative. It meets the acceptance criteria as the  
 261 moderator temperature is changed around the  
 262 (35°C-80°C). When moderator temperature is  
 263 changed, the fuel temperature is reminded  
 264 constantly. Table 4 showed that fuel temperature is  
 265 also negative when the fuel temperature was  
 266 changed around (50°C-200°C). Both parameters  
 267 (moderator and fuel coefficient of reactivity) are  
 268 significant for feedback reactivity for dynamic  
 269 analysis. The fuel temperature coefficient is a very  
 270 prompt effect because fuel temperature changes  
 271 quickly in a change in power. In an accident where  
 272 the power increases, a negative fuel temperature  
 273 reactivity coefficient provides a prompt negative  
 274 feedback, which tends to bring power down.

275 Table 3. Moderator temperature reactivity  
276 coefficient

Moderator temperature [°C]	k-eff [%Δk/k]	Core reactivity [ρ] [%Δk/k]	Δρ [%Δk/k]	Moderator reactivity coefficient [(%Δk/k)/°C]
35	1.035108	3.39188	0	-
45	1.034265	3.31313	-0.07875	-7.876E-03
60	1.032981	3.19296	-0.12019	-8.013E-03
80	1.031249	3.01865	-0.17431	-8.751E-03

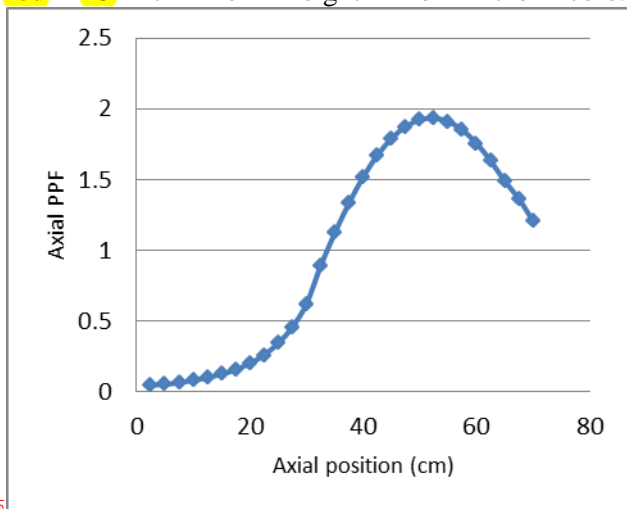
277

278 Table 4. Fuel temperature reactivity coefficient

Fuel Temperature [°C]	k-eff [%Δk/k]	Core reactivity [ρ] [%Δk/k]	Δρ [%Δk/k]	Fuel reactivity Coefficient [(%Δk/k)/°C]
50	1.044953	4.30201	0	-
100	1.043889	4.20448	-0.09753	-1.9506E-03
150	1.042898	4.11343	-0.09105	-1.8210E-03
200	1.042329	4.06118	-0.05225	-1.0450E-03

279

280 Figure 6 shows axial power peaking factor for  
281 hottest channels resulting from the calculation as the  
282 reactor operates at power of 50 MW. The maximum  
283 value of axial PPF is 1.9 as the position of control  
284 rod 25 cm of height from the core.



285

286 Fig. 6. Maximum axial power densities in D-2 core  
287 grid position

288

289 **C. Integral and differential control rod worth**

290

291 Reduction or increment of thermal utilization factor  
292 (f) is an important property of a control rod and  
293 depends on keff, whether the rod is inserted or  
294 withdrawn from the core. The change in Keff results  
295 in a change in the reactivity of the core. The worth  
296 of a control rod directly relates to its effect on  
297 reactivity and it has usually the same unit of that.  
298 The effectiveness, or worth, of a control rod,  
299 depends on mostly of the value of the neutron flux  
300 at the location of the rod. The change in reactivity  
301 caused by control rod motion is referred to as  
302 control rod worth. For a reactor with a single control

303 rod like MTR type reactor, the control rod's worth  
304 has a maximum effect if placed in the center of  
305 reactor core having the maximum flux. The  
306 difference of the worth of the rod between the  
307 inserted or withdrawn rod from the reactor is  
308 dependent on the axial flux shape. Generally, the  
309 flux at the top and bottom of the reactor is typically  
310 less than that in the middle. Therefore, the rod worth  
311 per unit length of the control rod at the top and  
312 bottom of the core is less than that in the middle  
313 during insertion or withdrawal. This behavior is  
314 typically illustrated in the integral and differential  
315 rod worth curves as shown in Figures 7 and 8  
316 respectively.

317

318 The integral control rod worth curve is particularly  
319 significant in research reactor operation. For a  
320 reactor which has a large amount of excess  
321 reactivity, several control rods are required [16]. To  
322 gain the full effectiveness of the rods and a  
323 relatively even flux distribution, the rods need to be  
324 distributed appropriately. The exact worth of each  
325 control rod is dependent upon the design of the  
326 reactor. The exact effect of control rods on reactivity  
327 can be usually estimated. For example, a control rod  
328 can be withdrawn in small increments, such as 5 cm,  
329 and the change in reactivity can then be determined  
330 following each increment of withdrawal. By plotting  
331 the resulting reactivity versus the rod position, a  
332 graph similar to that in Figure 7 is obtained. The  
333 graph depicts integral control rod worth over the full  
334 range of withdrawal. The integral control rod worth  
335 is the total reactivity worth at that particular degree  
336 of withdrawal and that is mostly defined to be the  
337 greatest if the rod fully withdrawn.

338

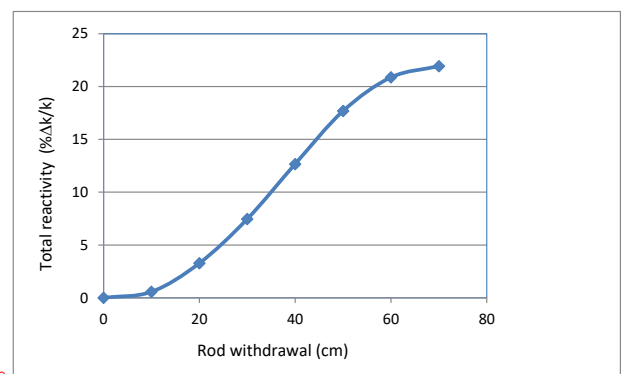
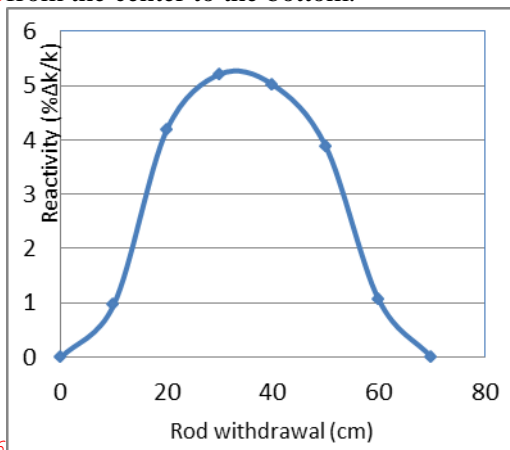


Fig 7. Integral control rod worth

342 The above Figure 7 shows that the gradient of the  
343 curve (Δρ/Δx) indicating the amount of reactivity  
344 inserted per unit of withdrawal is the highest when  
345 the control rod is mid out of the core. This occurs  
346 due to the area of the highest neutron flux near the  
347 center of the core. Therefore, the change of neutron  
348 absorption is the most one in this area. If the slope

349of the curve for integral rod worth in Fig. 7 is taken 393burn-ups of neutron absorber, follower fuel and  
 350into account, the rate of change of control rod worth 394distribution of fuels in the reactor core.  
 351will then be the function of control rod position. 395

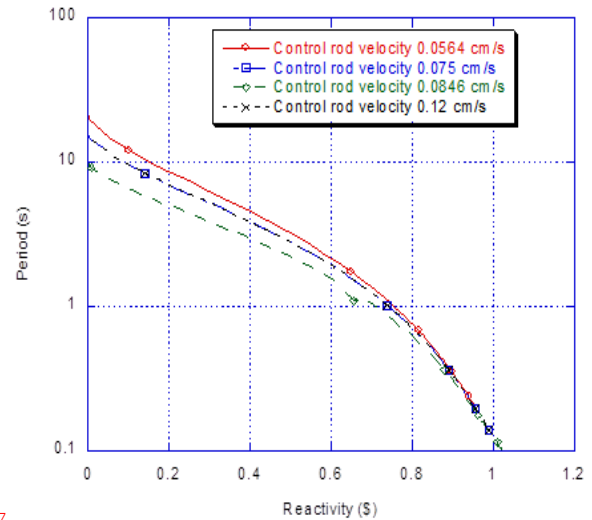
352A plot of the slope of the integral rod worth curve, 396  
 353so called the differential control rod worth, is then 397  
 354shown in Fig. 8. It is seen that at the bottom of the 398  
 355core, where there are few neutrons, the rod 399  
 356movement has little effect due to the little various 400  
 357change in reactivity worth per cm. As the rod 401  
 358approaches the center of the core, its effect becomes 402  
 359greater, and hence making the change in reactivity 403  
 360worth per unit length greater. However, at the center 404  
 361of the core, the differential rod worth is the highest 405  
 362depending on small rod motion. From the center of 406  
 363the core to the top, the rod worth per unit length is  
 364basically inversed to the rod worth per unit length  
 365from the center to the bottom.



366  
 367Fig 8. Differential of control rod worth

368  
 369The control fuel element (CFE) are modeled in  
 370Batan-3DIFF code and based on the code, XS  
 371requirements, four groups of neutron energy for  
 372libraries of XS are provided. This was only done by  
 373changing the thermal capture cross-section of a  
 374region of concern by an amount such that the  
 375reactivity of inserted control rod would correspond  
 376to the benchmark. The control rod worth is  
 377estimated by calculating keff with all four absorber  
 378boxes inserted in the core. The results are shown in  
 379Fig. 7 indicating the axial power shape as a function  
 380of the control position in the reactor ranging from  
 381fully inserted to fully withdrawn positions. An axial  
 382peaking factor of 1.5 is obtained bounded by the  
 383limit. The effect of the insertion rate on the flux  
 384density is illustrated in Fig 7. In addition, Fig 8  
 385shows the worth of fully inserted four control fuel  
 386elements. The result shows that the gradient is 0.594  
 387%Δk/k/cm and by adding 15 % of the safety factor,  
 388that becomes 0.68 %Δk/k/cm. From Fig 8 showing  
 389the differential worth of control fuel elements, it can  
 390be said that the most effective control rod is at the  
 391position of 25-40 cm. In addition, the following  
 392factors surely affect the control rod worth, such as,

**d. Period- reactivity relation**  
 397To calculate the control rod velocity is used  
 398POKDYN program. POKDYN program written in  
 399Fortran consisting of main program, POKS  
 400subroutine, POKIN subroutines, and Function  
 401REACH Function that uses kinetic equations point  
 402to complete the calculation in terms of neutronic  
 403transient conditions and accidents because of  
 404reactivity insertion. The results of the calculations  
 405of period-reactivity relationship using the data of  
 406Table 2 , Table 3 and Table 4.



407  
 408 Fig 9. Maximum control rod speed

409  
 410Reactivity can not be directly measurable and in  
 411most research reactors, procedures do not refer to it  
 412and most technical specifications do not limit it.  
 413Instead, they specify a limiting rate of neutron  
 414power rising (measured by detectors), commonly  
 415called a reactor period (especially in the case of  
 416MTR type reactor). The smaller the value of  $\tau_e$ , the  
 417more rapid the change in reactor power. The reactor  
 418period may be positive or negative. As the reactor  
 419period is positive, reactor power increases or vice  
 420versa. If the reactor period is constant with time, as  
 421associated with exponential power change, the rate  
 422is referred to as a stable reactor period. However, if  
 423the reactor period is not constant but is changing  
 424with time, as for non-exponential power change, the  
 425period is referred to as a transient reactor period.  
 426According to German system (SUS), once reactor  
 427period (reactor doubling time) < 10 s, power  
 428increases fast and power scram is set [16].  
 429A much more exact formula reactor period is based  
 430on solutions of six-group point kinetics equations.  
 431From these equations, an equation, called the in-  
 432hour equation (which comes from the inverse hour,  
 433when it was used as a unit of reactivity that

434 corresponded to e-fold neutron density change 490 Sometime, it is difficult to measure cladding or fuel  
 435 during one hour), may be derived. The reactor 491 temperature in a research reactor. Thus, the  
 436 period,  $\tau_e$ , or e-folding time, is defined as the time 492 calculated temperatures are used to evaluate the  
 437 required for the neutron density to change by a 493 consequences of an accident. During the accident,  
 438 factor  $e = 2.718$ . The reactor period is usually 494 the calculated maximum fuel and cladding  
 439 expressed in units of seconds or minutes. On the 495 temperature of the central channel amount to  $196^\circ\text{C}$   
 440 MTR type research reactor the acceptance criteria 496 and  $192^\circ\text{C}$  respectively. Thus, the maximum clad  
 441 for a period  $> 10$  s, so the Fig 9 showed the relation 497 temperature is far from the fuel temperature safety  
 442 of period and reactivity for MTR type research 498 limit of  $210^\circ\text{C}$ , ensuring that no sub-cooled boiling  
 443 reactor. The result showed that for control rod speed 499 occurs. Hence, the transient indicates that the  
 444  $0.0564$  cm/s, the period more than 10 s. If the speed 500 accomplished power peak of about 66 MW does not  
 445 of the control rod changes to  $0.075$  cm/s, the period 501 affect the fuel elements, since no DNB is to be  
 446 of the core is still more than 10 s. This also the same 502 expected under these conditions  
 447 as that changes to again to  $0.0846$ . However, when 503 During RIA events, the core becomes  
 448 the speed of the control rod increases to  $0.12$  m/s, 504 supercritical and generally core power rises to level  
 449 the period becomes less than 10 s. This means that 505 beyond the heat removal system capability. For this  
 450 the maximum control rod for the MTR type research 506 reason, such events are considered one of the most  
 451 reactor is  $0.0846$  cm/s. 507 severe transients that could lead to core damage. To  
 452 508 understand the dynamics of such phenomena, it is  
 453 e. Thermal-hydraulics and dynamics analysis 509 necessary to identify the various key parameters that  
 454 510 govern the power excursion shape, the inherent self-  
 455 The coolant mass flow rate in the MTR type 511 limiting behavior, the power, and the released  
 456 research reactor is limited by the flow instability 512 energy. These later are mainly governed by the  
 457 phenomenon. Reactor with high thermal power can 513 prompt neutron lifetime **that** used in the core. There  
 458 occur flow instability characterized by a flow 514 are also the delayed neutron fraction, reactivity  
 459 excursion. **When the flow rate and the heat flux are** 515 coefficient related to complex interactions of the  
 460 **relatively high, a small increase in heat flux causes a** 516 physical process between kinetics and thermal-  
 461 **sudden large decrease in flow rate.** For higher 517 hydraulics phenomena as well as the response of the  
 462 uranium density, the thickness of the plate or the 518 reactor control system. The MTR type research  
 463 channel width is increased so that the reactor is 519 reactor core with 390 gram of fuel loading  
 464 stable at a high flow rate. In addition to reducing the 520 corresponds to ramps reactivity of 51 pcm/s. In this  
 465 heat flux in the fuel, it can be done by the higher of 521 case, the role of prompt (Doppler reactivity) and  
 466 fuel height so the maximum temperature of fuel and 522 delayed coolant temperature rise feedback effects  
 467 cladding will be reduced. Based on the calculation, 523 and they are emphasized in all the consideration  
 468 the maximum coolant flow rate obtained at 900 524 transients. The scram system is activated when the  
 469  $\text{kg/m}^2\text{s}$ . By using the mass flow in the core is 900 525 reactor power reaches at 59 MW. Since there is  $0.5$   
 470  $\text{kg/s}$ , the maximum coolant velocity at fuel channel 526 seconds to actualizing the control rod scram system,  
 471 is  $12.29$  m/s. 527 the power increases to 66 MW. When the reactor  
 472 Starting from the initial conditions of  $45^\circ\text{C}$  for 528 power increases to 66 MW, the fuel, cladding, and  
 473 core temperature and  $0.02\%$  of nominal for the 529 coolant temperatures are  $196^\circ\text{C}$ ,  $192^\circ\text{C}$ ,  $76^\circ\text{C}$   
 474 power (1 MW), a ramp reactivity of 51 pcm/s was 530 respectively, but they are still below the safety limit  
 475 inserted during 16 sec. The fuel and moderator 531 of  $210^\circ\text{C}$ . The temperature of the fuel, coolant and  
 476 temperature feedback coefficient of reactivity are 532 cladding should be limited to maintain the integrity  
 477 noted in Table 3 and Table 4. Figure 10 and Figure 533 of the fuel. Table 5 showed that the maximum  
 478 11 show the development of calculated relative 534 temperature in the fuel, cladding, and moderator. It  
 479 reactor power and average core temperature. The 535 was stated that reactions of  $\gamma\text{UMo}$  alloys with  
 480 comparison to the safety limit  $210^\circ\text{C}$  of maximum 536 aluminum started typically at the temperature of  
 481 fuel temperature depicts good calculation result 537  $645^\circ\text{C}$  [17]. It is also indicated a temperature of  
 482 compared with safety limit. Starting from the initial 538  $641^\circ\text{C}$  for the melting point of the aluminum, and it  
 483 value the power increases to about 66 MW of 539 is suggested that chemical reaction started soon after  
 484 power, the average core temperature escalates to 540 the melting phenomena. Thus, it is confirmed the  
 485 about  $76^\circ\text{C}$ . This behaviour stimulates the negative 541 validity of the fundamental assumptions of their  
 486 reactivity feedback effect that is able at this point to 542 approach to the detection of possible reactions in the  
 487 consume the entire available excess reactivity 543 U-Mo-Al system. The formation of a layer of liquid  
 488 forcing the power to decrease and demonstrating the 544 aluminum in contact with the  $\gamma\text{UMo}$  particles  
 489 inherently safety features of conceptual reactor core. 545 promotes an effective contact between both

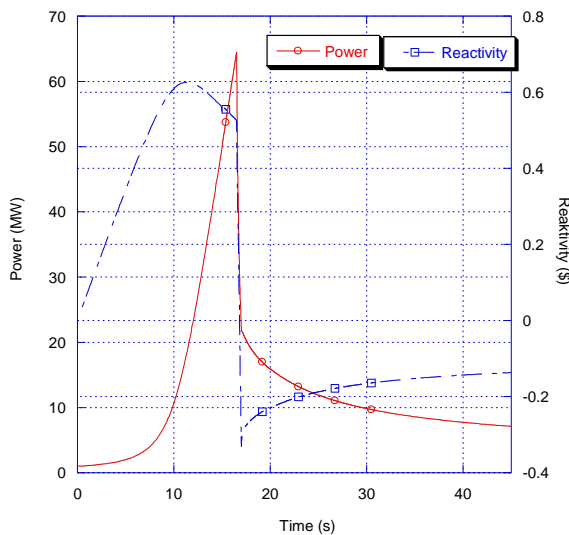
546surfaces, enhancing the probability of reaction. So  
 547the fuel and cladding temperature are still far below  
 548the melting point of the aluminum as a cladding.

549 Figure 10 showed the power and reactivity  
 550profile after insertion of reactivity 51 pcm/s and  
 551after 16 seconds the maximum power reached 66  
 552MW and then reactor scram by setting point at 118  
 553% of maximum power. Figure 11 showed the  
 554temperature profile of fuel, cladding, and  
 555moderator. The maximum temperature is still below  
 556the safety limit for U-9Mo/Al fuel.

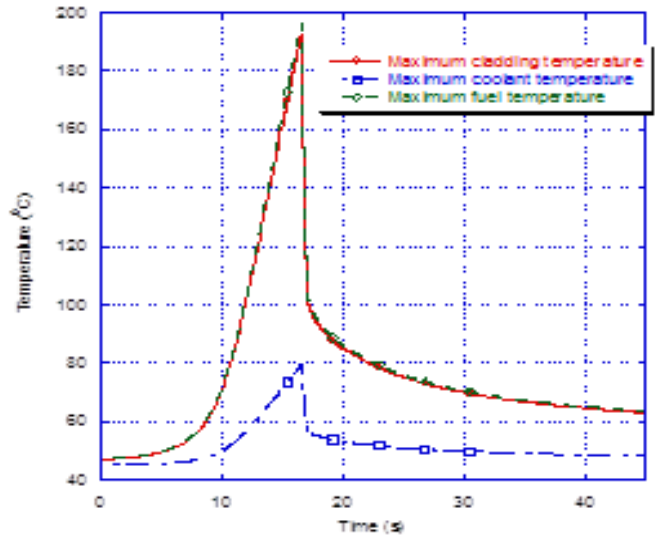
557Table 5. Maximum temperature with various  
 558uranium density at fuel elements

Parameters	Uranium density [3.96 gram/cm <sup>3</sup> ]
Coolant temperature at core inlet [°C]	44.5
Coolant temperature at core outlet [°C]	60.50
Maximum temperature at coolant [°C]	76.0
Maximum temperature at cladding [°C]	192.0
Maximum temperature at fuel meat [°C]	196.0

559



560  
 561Fig 10. Power and reactivity of the core as transient  
 562



563  
 564

565Fig 11. Maximum fuel, cladding and moderator  
 566temperatures

567

568**CONCLUSIONS**

569

570Core configuration including a number of in-core  
 571irradiation positions has a very much influence on  
 572the value and distribution of neutron fluxes either  
 573in-core or reflector region. To have an increase of  
 574neutron flux in the core region, it can be obtained by  
 575adding an in-core irradiation position. The outer  
 576irradiation positions have the biggest influence on  
 577increasing the neutron flux in the reflector region.  
 578For the MTR type research reactor, based on the  
 579equilibrium core, the best core is using fuel density  
 580of 3.96 gram/cm<sup>3</sup> that provides so many irradiation  
 581positions with highest neutron fluxes. Based on the  
 582calculation of MTR-DYN code, it is clear that  
 583uranium densities of 3.96 for U9Mo-Al fuel that are  
 584proposed in this research work can be utilized as a  
 585candidate fuel for the RRI reactor core. The  
 586neutronics and thermal-hydraulics criteria are  
 587fulfilled with no exceeding safety limit. Fuel  
 588cladding strain limit is not exceeding during  
 589anticipated transient with a thermal power of 50  
 590MW. The dynamic characteristic of the core has to  
 591carry out with a core configuration of 3.96 gram/cm<sup>3</sup>  
 592at optimum uranium density of U9Mo-Al fuel for  
 593MTR research reactor without safety rod which  
 594proposed in this research can be applied with good  
 595safety features.

596

597**ACKNOWLEDGMENT**

598

599The authors wish to express special thanks to Dr.  
 600Jupiter S. Pane MSc. and Ir. Tagor Malem  
 601Sembiring for his fruitful discussions and to Dr.  
 602Geni Rina Sunaryo, heat of PTKRN for her support  
 603and also thank you to the Management of PTKRN.

604 This research was funded from the DIPA PTKRN 638  
 605 Year 2010-2014 639

606 640

607 **REFERENCES** 641

608 642

609 1. F. Muhammad, A. Majid, Progress in 643  
 610 Nuclear Energy 51 (2009) 339. 644

611 <http://dx.doi.org/10.1016/j.pnucene.2008.06.003> 645

612 2. T. Surbakti, S. Pinem, T. M. Sembiring, et 646  
 613 al., Tri Dasa Mega 3 3 (2012) 179. 647

614 3. I. Kuntoro, T. M. Sembiring, Tri Dasa Mega 648  
 615 16 1 (2014) 1. 649

616 4. H. Kazeminejad, Annals of Nuclear Energy 650  
 617 45 (2012) 59. 651

618 <http://dx.doi.org/10.1016/j.anucene.2012.02.017> 652

619 5. I. D. Abdelrazek, M. Naguib Aly, A. A. 653

620 Badawi, et al., Annals of Nuclear Energy 70 654  
 621 (2014) 36. 655

622 [http://dx.doi.org/10.1016/j.anucene.2014.02.](http://dx.doi.org/10.1016/j.anucene.2014.02.023) 656

623 023 657

624 6. X. Shen, K. Nakajima, H. Unesaki, et al., 658  
 625 Ann. Nucl. Energy 62 (2013) 195. 659

626 [http://dx.doi.org/10.1016/j.anucene.2013.06.](http://dx.doi.org/10.1016/j.anucene.2013.06.014) 660  
 627 014. 661

628 7. M. A. Albatia, S. O. AL-Yahiaa, J. Park, et 662

629 al., Prog. Nucl. Energy 71 (2014) 1 663

630 [http://dx.doi.org/10.1016/j.pnucene.2013.10](http://dx.doi.org/10.1016/j.pnucene.2013.10.015) 664

631 .015 665

632 8. D. Jo, J. Park, H. Chae, Prog. Nucl. Energy 666

633 71 (2014) 39 667

634 [http://dx.doi.org/10.1016/j.pnucene.2013.11](http://dx.doi.org/10.1016/j.pnucene.2013.11.006) 668

635 .006 669

636 9. S. Pinem, T. M. Sembiring, Setiyanto, Tri 670

637 Dasa Mega 11 3 (2009) 153. 671

638 672

639 673

10. T. Surbakti, T. M. Sembiring, Tri Dasa 638  
 Mega 18 1 (2016) 29. 639

11. L. Suparlina, T. Surbakti, Tri Dasa Mega 640  
 16 2 (2014) 89. 641

12. S. Pinem, T.M. Sembiring, P.H. Liem, 642  
 Atom Indonesia Vol. 42 No. 3 (2016) 123. 643

<http://dx.doi.org/10.17146/aij.2016.532>. 644

13. Rokhmadi, T. Surbakti, Tri Dasa Mega 15 645  
 2 (2012) 77. 646

14. A. Hedayat, Prog. Nucl. Energy 71 (2014) 647  
 61. [http://dx.doi.org/10.1016/S0149-1970](http://dx.doi.org/10.1016/S0149-1970(14)00018-3) 648

(14) 00018-3 649

15. S. Pinem, I. Kuntoro, Teknologi Bahan 650  
 Nuklir 10 1 (2014) 1. 651

16. R. Nasira, M. K. Butt, S. M. Mirzac, et al., 652  
 Ann. Nucl. Energy 85 (2015) 869. 653

[http://dx.doi.org/10.1016/j.anucene.2015.07.](http://dx.doi.org/10.1016/j.anucene.2015.07.003) 654  
 003. 655

17. H. J. Ryu, Y. S. Kim. Nucl. Eng 656  
 Technology 46 (2014) 159. 657

<http://dx.doi.org/10.5516/NET.07.2014.705> 658

